International Conference on Control, Engineering & Information Technology (CEIT'13)
Proceedings Engineering & Technology - Vol.1, pp.93-98, 2013

An IRFOC Drive Scheme for a SEIG-Wind Turbine Water Pumping System

Noureddine Hidouri[1] and Lassâad Sbita[2]

[1]noureddine.hidouri@yahoo.fr, [2]lassaad.sbita@enig.rnu.tn

Research Unit of Photovoltaic, Wind turbine and Geothermal Systems

National Engineering School of Gabes, Tunisia

Abstract— **In this paper, the authors present an IRFOC drive scheme for an isolated wind turbine water pumping system. The turbine is used to drive the Self Excited Induction Generator (SEIG) in order to feed an isolated load composed of an induction motor and a hydraulic centrifuge pump. The considered load receives the required active power from the SEIG through a diode rectifier, a buck converter and an inverter. The models of the wind turbine, the SEIG, the diode rectifier, the buck converter, the inverter and the centrifuge pump are developed and used in the control scheme. The dynamic performances of the turbine, the generator and the motor are analyzed. The simulation results have shown that the proposed methodology is an efficient solution of an important control system.**

Keywords**— wind turbine, water pumping system, FOC, SEIG, Induction motor.**

I. INTRODUCTION

In the isolated areas as the rural zones, the islands and the mountains, the use of the renewable energy such as photovoltaic and the wind energy is a improved solution for such applications as the electrification and the water pumping system [1-4].

Many category of electric generators have been associated with wind turbines and proposed to convert wind power into electric power such as PMSG [5],[6], DFIG [7-10], IG [1], [2],[11].

Different types of motors are used in water pumping system. PMSM [12],[13], IM are also used in the pumping system applications with several control strategies [14],[15].

Many techniques of control have been applied to induction motor as direct torque control (DTC) and field oriented control. The concept of field oriented control (FOC) is firstly developed by Blasche,[16]. The FOC is a flux-torque decoupling technique applied to AC machines. Two approaches are possible: the direct field orientation (DFO) based on the rotor flux angle given by a flux observer or estimator and the indirect field orientation (IFO) based on the rotor slip calculation, [17], [18].

In this paper an indirect rotor field oriented control is synthesized for an induction motor (IM) associated to an isolated wind turbine water pumping system in order to generate the torque required by the centrifuge pump load.

II. THE WIND WATER PUMPING SYSTEM MODEL

Figure 1 shows the proposed wind turbine water pumping system considered in this paper. The rotor of the pitch controlled wind turbine is coupled to a Self Excited Induction Generator (SEIG) through a gear-box in order to convert the mechanical power to electric power. The produced SEIG supply is converted by the diode rectifier, filtered by an LC filter, converted by an inverter and used to feed an IRFOC controlled induction motor that is coupled to a hydraulic centrifuge pump.

A. Turbine Model

The will known power coefficient $C_p(\beta,\lambda)$ of the horizontal axis wind turbine used is this research work is a nonlinear function of the tip speed ration λ and the pitch angle β. It is given by relation (1) where c_1 to c_6 represents the turbine characteristic coefficients, [20], [21].

$$\begin{cases} C_p(\beta,\lambda) = c_1\left(\frac{c_2}{\lambda_i} - c_3\beta - c_4\right)e^{-\frac{c_5}{\lambda_i}} + c_6\lambda \\ \frac{1}{\lambda_i} = \frac{1}{\lambda + 0.008\beta} - \frac{0.035}{\beta^3+1} \end{cases} \quad (1)$$

The tip-speed ratio used in relation (1) is expressed by the following relation:

$$\lambda = \frac{R\Omega_T}{v_w} \quad (2)$$

The mechanical power extracted by a wind turbine from the wind and the developed turbine torque are respectively given by the well-known formulas (3) and (4).

$$P_T = \frac{1}{2}\rho A C_p(\beta,\lambda) v_w^3 \quad (3)$$

$$C_T = \frac{1}{2}\rho\pi R^3 \frac{C_p(\beta,\lambda)}{\lambda} v_w^2 \quad (4)$$

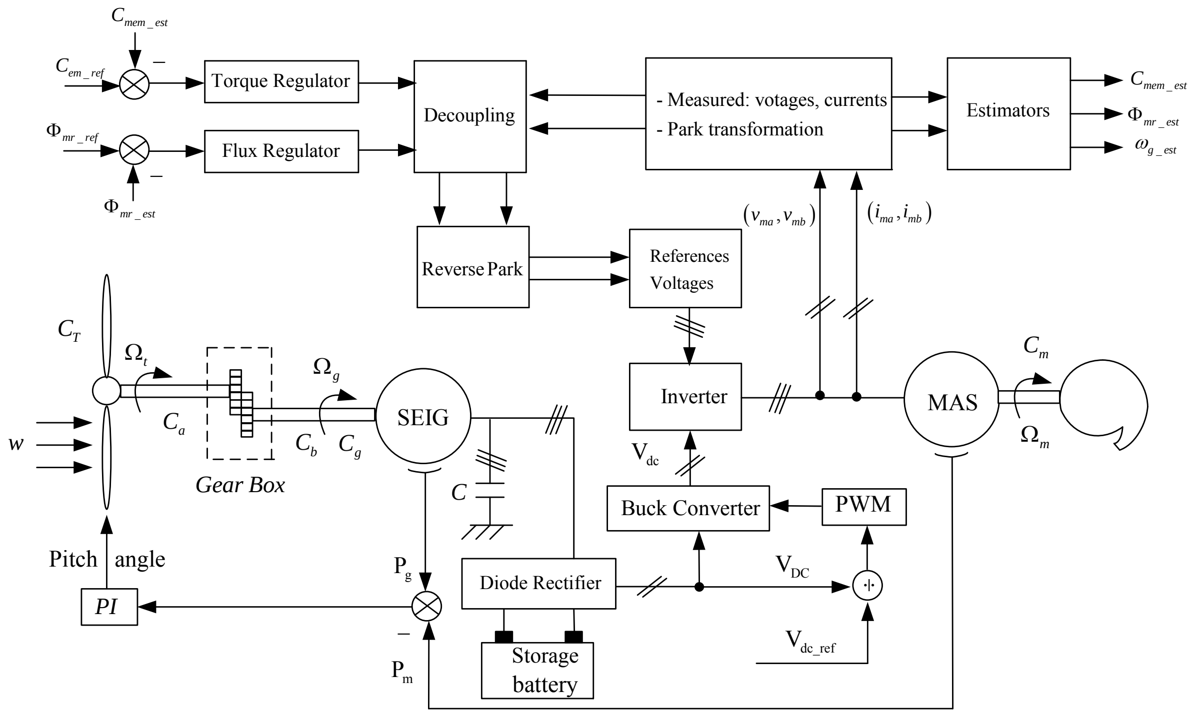

Fig. 1 Proposed wind turbine pumping system

B. SEIG complex model

In the Concordia stationary reference frame, applied to the SEIG stator, the Ohm's law is given by:

$$\bar{v}_{gs} = -R_s \bar{i}_{gs} + \frac{d\bar{\varphi}_{gs}}{dt} \quad (5)$$

The stator flux vector $\bar{\varphi}_{gs}$ is linked to the stator current $\bar{i}_{gs}$ and rotor flux $\bar{\varphi}_{gr}$ by the equation (6):

$$\bar{\varphi}_{gs} = -\sigma L_s \bar{i}_{gs} + \frac{M_{sr}}{L_r}\bar{\varphi}_{gr} \quad (6)$$

The magnitude Φ_{gs} of the stator flux vector $\bar{\varphi}_{gs}$ and the magnitude Φ_{gr} of the rotor flux vector $\bar{\varphi}_{gr}$ are constant; consequently, the vectors:

$$\begin{cases} \bar{\varphi}_{gs} = \Phi_{gs} e^{j\theta_{gs}} \\ \bar{\varphi}_{gr} = \Phi_{gr} e^{j(\theta_{gs}-\theta_{gr})} \end{cases} \quad (7)$$

The expression of the magnetizing inductance with consideration of the phase voltage is given by relation (8), [19].

$$M_{sr} = -1.62e^{-11}.V_{ph}^4 + 2.67e^{-8}.V_{ph}^3 - 1.38e^{-5}.V_{ph}^2 + 1.76e^{-3}.V_{ph} + 0.23 \quad (8)$$

The leakage inductances of stator and rotor are given by the following formula:

$$\begin{cases} \ell_s = L_S - M_{sr} \\ \ell_r = L_r - M_{sr} \end{cases} \quad (9)$$

The capacitor voltage vector is equal to the stator voltage vector and expressed by relation (10):

$$\bar{V}_C = \bar{v}_s = \frac{1}{C}\int \bar{i}_C dt + \bar{V}_{C0} \quad (10)$$

The generator electromagnetic torque is given by (11) where p_g represents the SEIG pair pole number.

$$C_{gem} = \frac{p_g M_{sr}}{\sigma L_s L_r} \bar{\varphi}_{gs} \wedge \bar{\varphi}_{gr} \quad (11)$$

The mechanical system of the wind turbine system can be described by the simplified motion equation:

$$C_T - C_{gem} = J_{tg}\frac{d\Omega_T}{dt} + f_{tg}\Omega_T \quad (12)$$

C. Induction Motor Model

In the Concordia stationary reference frame, applied to the induction motor stator, the Ohm's law is given by:

$$\overline{v}_{ms} = R_s \overline{i}_{ms} + \frac{d\overline{\varphi}_{ms}}{dt} \qquad (13)$$

The stator flux vector $\overline{\varphi}_{ms}$ is linked to the stator current $\overline{i}_{ms}$ and rotor flux $\overline{\varphi}_{mr}$ by the equation (14):

$$\overline{\varphi}_{ms} = \sigma L_s \overline{i}_{ms} + \frac{M_{sr}}{L_r}\overline{\varphi}_{mr} \qquad (14)$$

The magnitude Φ_{ms} of the stator flux vector $\overline{\varphi}_{ms}$ and the magnitude Φ_{mr} of the rotor flux vector $\overline{\varphi}_{mr}$ are constant; consequently, the vectors:

$$\begin{cases} \overline{\varphi}_{ms} = \Phi_{ms} e^{j\theta_{ms}} \\ \overline{\varphi}_{mr} = \Phi_{mr} e^{j(\theta_{ms}-\theta_{mr})} \end{cases} \qquad (15)$$

The electromagnetic torque can be expressed by relation (16) where p_m represents the motor pair pole number.

$$C_{mem} = \frac{p_m M_{sr}}{\sigma L_s L_r}\overline{\varphi}_{ms} \wedge \overline{\varphi}_{mr} \qquad (16)$$

When Park synchronous reference frame with the stator flux is used, (13) becomes as follows, where ω_s is the electric stator flux speed:

$$\overline{V}_{ms} = R_s \overline{I}_{ms} + \frac{d\overline{\Phi}_{ms}}{dt} + j\omega_s \overline{\Phi}_{ms} \qquad (17)$$

The stator flux and the rotor flux vectors are linked to those of current vector by:

$$\begin{cases} \overline{\Phi}_{ms} = L_s \overline{I}_{ms} + M_{sr}\overline{I}_{mr} \\ \overline{\Phi}_{mr} = M_{rs}\overline{I}_{ms} + L_r \overline{I}_{mr} \end{cases} \qquad (18)$$

The electromagnetic torque can be expressed by:

$$C_{mem} = p_m \frac{M_{sr}}{L_r}(\Phi_{mrd} I_{msq} - \Phi_{mrq} I_{msd}) \qquad (19)$$

D. Centrifugal pump model

The centrifugal pump model can be described by the will known mechanical characteristic illustrated in relation (20).

$$h = a_0\omega_r^2 - a_1\omega_r Q - a_2 Q^2 \qquad (20)$$

The hydraulic power P_H and the load torque of the centrifugal pump can be described respectively by (21) and (22).

$$P_H = \rho g Q H \qquad (21)$$

$$C_r = k_r \Omega^2 + C_s \qquad (22)$$

The mechanical model of the electric motor can be described by (23) where f_m and C_r represent respectively the motor's friction coefficient and the hydraulic load torque of the centrifugal pump.

$$C_{em} = J_m \frac{d\Omega_m}{dt} + f_m \Omega_m + C_r \qquad (23)$$

E. Buck Converter Model

The schematic of the buck converter power stage that provides a stepped-down voltage to the load is given in fig. 2

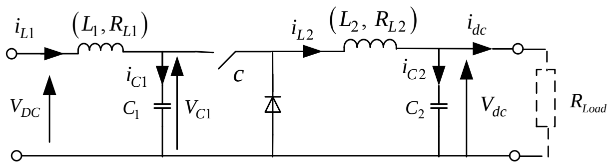

Fig. 2 Structure of the buck converter

We designate by c a Boolean variable that takes the value $(c = 0)$ if the key is switched off and the diode is switched on and takes the value $(c = 1)$ if the key is switched on and the diode is switched off. Thus, the model is given as, [10]:

$$\begin{bmatrix} \dot{i}_{L1} \\ \dot{i}_{L2} \\ \dot{V}_{c1} \\ \dot{V}_{c2} \end{bmatrix} = \begin{bmatrix} -\frac{R_{L1}}{L_1} & 0 & -\frac{1}{L_1} & 0 \\ 0 & -\frac{R_{L2}}{L_2} & \frac{c}{L_2} & -\frac{1}{L_2} \\ \frac{1}{C_1} & -\frac{c}{C_1} & 0 & 0 \\ 0 & \frac{1}{C_2} & 0 & -\frac{1}{R_{Load}C_2} \end{bmatrix} \begin{bmatrix} i_{L1} \\ i_{L2} \\ V_{C1} \\ V_{C2} \end{bmatrix} + \begin{bmatrix} \frac{1}{L_1} \\ 0 \\ 0 \\ 0 \end{bmatrix} V_{DC} \qquad (24)$$

$$V_{dc} = \begin{bmatrix} 0 & 0 & 0 & 1 \end{bmatrix} \begin{bmatrix} i_{L1} & i_{L2} & V_{C1} & V_{C2} \end{bmatrix}^t \qquad (25)$$

III. THE IM FIELD-ORIENTED CONTROL STRATEGY

After arrangement, equation (17) can be represented by (26) where the different related terms are given by (27).

$$\overline{V}_{ms} = \overline{V}_{s1} - \overline{E} \qquad (26)$$

$$\begin{cases} \overline{V}_{s1} = \sigma L_s \frac{d\overline{I}_{ms}}{dt} + \left(R_s + R_r \frac{M_{sr}^2}{L_r^2}\right)\overline{I}_{ms} \\ \overline{E} = \frac{M_{sr}R_r}{L_r^2}\overline{\Phi}_{mr} - j\left[\sigma L_s \omega_s \overline{I}_{ms} + \frac{M_{sr}\omega_r}{L_r}\overline{\Phi}_{mr}\right] \end{cases} \qquad (27)$$

Considering the rotor flux orientation condition given by relation (28) and the famous relation (29), we can establish (30).

$$\begin{cases} \Phi_{mrd} = \Phi_{mr} \\ \Phi_{mrq} = 0 \end{cases} \quad (28)$$

$$\omega_s = \omega_r + \frac{M_{sr} R_r}{L_r \Phi_{mr}} I_{msq} \quad (29)$$

$$\begin{cases} E_d = \frac{M_{sr} R_r}{L_r^2} \Phi_{mr} + \sigma L_s \omega_s I_{msq} \\ E_q = -\sigma L_s \omega_s I_{msd} - \frac{M_{sr} \omega_s}{L_r} \Phi_{mr} + \frac{M_{sr}^2 R_r}{L_r^2} I_{msq} \end{cases} \quad (30)$$

A. Estimation of the rotor flux, the slip frequency and the electromagnetic torque

The rotor flux can be estimated from the direct stator current component obtained when the park transformation is applied to the measured three stator currents as indicated by the will known relation (31).

$$\Phi_{mr\_est} = \frac{M_{sr}}{1 + \frac{L_r}{R_r} p} I_{msd} \quad (31)$$

The slip frequency (32) is estimated from the quadratic current and the estimated rotor flux.

$$\omega_{g\_est} = \frac{M_{sr}}{\frac{L_r}{R_r} \Phi_{mr\_est}} I_{msq} \quad (32)$$

The expression of the estimated electromagnetic torque is given by relation (33).

$$C_{mem\_est} = p \frac{M_{sr}}{L_r} \Phi_{mr\_est} I_{msq} \quad (33)$$

B. Regulation of the electromagnetic torque

The torque transfer function torque/voltage is given by:

$$H_{Cem}(p) = \frac{C_{em}(p)}{V_{sq1}(p)} = \frac{p M_{sr} \Phi_{mr}}{L_r} \frac{\left[R_s + R_r \frac{M_{sr}^2}{L_r^2} \right]^{-1}}{1 + p\sigma L_s \left[R_s + R_r \frac{M_{sr}^2}{L_r^2} \right]^{-1}} \quad (34)$$

If the pole-zero cancellation method is used and the closed loop transfer function is assumed to a first order system characterized by an imposed response time equal to 5%, the expressions and the parameters of the PI torque controller can be expressed by (35).

$$\begin{cases} C_{cem}(p) = K_{p\_cem} \left(1 + \frac{1}{\tau_{cem} p} \right) \\ \tau_{cem} = \sigma L_s \left[R_s + R_r \frac{M_{sr}^2}{L_r^2} \right]^{-1} ; \; K_{p\_cem} = 3 \frac{\sigma L_r L_s}{p M_{sr} \Phi_{ref} t_r (5\%)} \end{cases} \quad (35)$$

C. Regulation of the rotor flux

The transfer function flux/current is given by:

$$H_{\Phi rd}(p) = \frac{\Phi_{mrd}}{I_{msd}} = \frac{M_{sr}}{1 + \frac{L_r}{R_r} p} \quad (36)$$

If the pole-zero cancellation method is used, the expressions and the parameters of the PI flux controller can be expressed by (37) .

$$\begin{cases} C_\Phi(p) = K_\Phi \left(1 + \frac{1}{\tau_\Phi p} \right) \\ K_\Phi = \frac{1}{M_{sr}} ; \; \tau_\Phi = \frac{L_r}{R_r} \end{cases} \quad (37)$$

IV. Simulation Results and Discussion

The simulation in this work has been developed in Matlab/Simulink environment.

In this study, we consider that the load is fed by the SEIG through a rectifier, a buck converter and an inverter (fig.1).

A. Wind turbine and SEIG analysis

Fig. 3 presents the proposed wind profile; it covers a speed range between 9 m/s and 12 m/s. The nominal wind turbine speed is equal to 9 m/s.

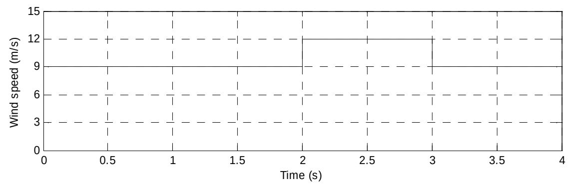

Fig. 3 Proposed wind profile

The pitch angle response is shown by fig. 4, it varies with the wind in order to adapt the SEIG power to the load power, it's important here to indicate that the load is applied at t = 1s.

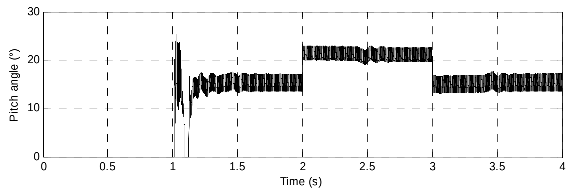

Fig. 4 Pitch angle response

Fig. 5 and fig. 6 give respectively the per-phase SEIG voltage response and the SEIG electromagnetic torque response. It's shown that SEIG voltage takes a sinusoidal shape and reaches the nominal value when the nominal load is applied. The electromagnetic torque converges to the nominal value at the nominal conditions.

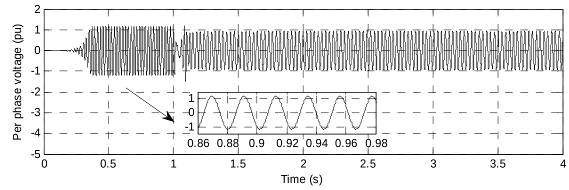

Fig. 5 Per phase SEIG voltage response

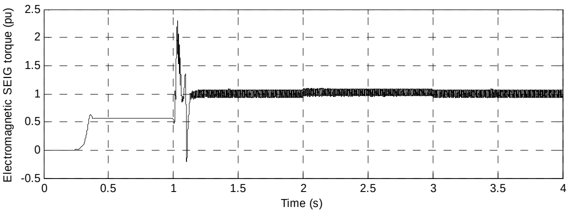

Fig. 6 SEIG electromagnetic torque response

B. *Analyses of physical sizes relating to the diode rectifier and the buck converter*

The output diode rectifier voltage is given by fig.7. This signal is filtered and will be adapted to the load by the buck converter.

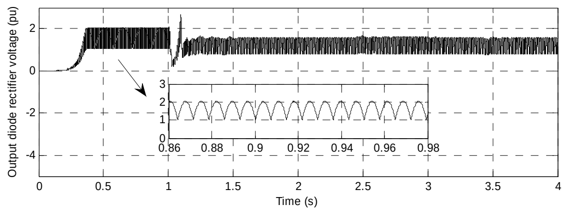

Fig. 7 Per phase voltage response

The command of the buck converter is based on the DC voltage required by the load. This value is computed as a reference buck voltage term. Fig.8 and fig.9 give respectively the input and the output buck converter voltages, the second one (fig. 9) converges towards the required DC voltage according to the first one.

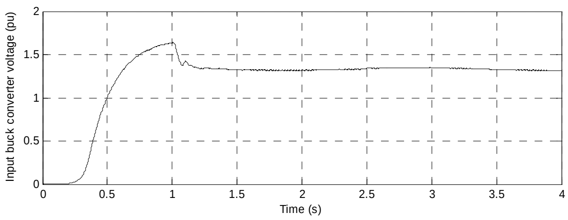

Fig. 8 Input buck converter voltage

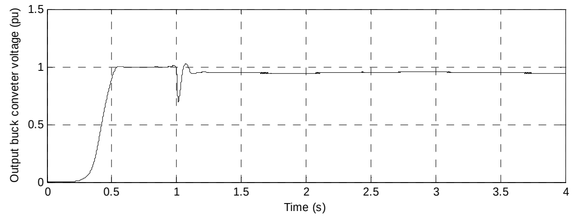

Fig. 9 Output buck converter voltage

C. *Analyses of physical sizes relating to the induction motor*

Initially, the induction motor is at stopped, at $t = 1s$, a reference direct rotor flux and a reference electromagnetic torque was applied to the motor.

The reference and estimated direct rotor fluxes are respectively given by figure 10 and figure 11. It's shown that the estimated converges strictly to the reference one.

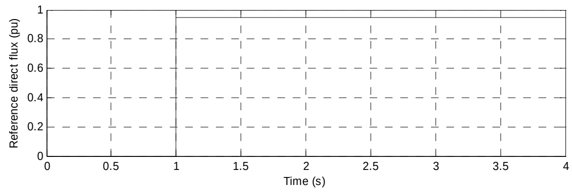

Fig. 10 Reference direct rotor flux

Related to fig. 11 (estimated direct rotor flux), figure 12 shows that the quadratic component rotor flux converges to zero as an improvement that the rotor flux is oriented to the direct axis. The reference electromagnetic torque (fig.13) as well as the estimated electromagnetic torque (fig.14) converge towards their target ones (rated values).

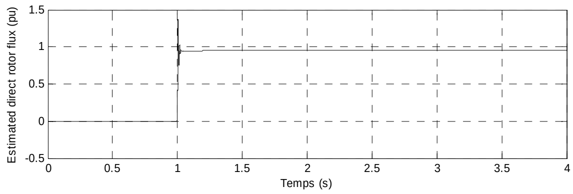

Fig. 11 Estimated direct rotor flux

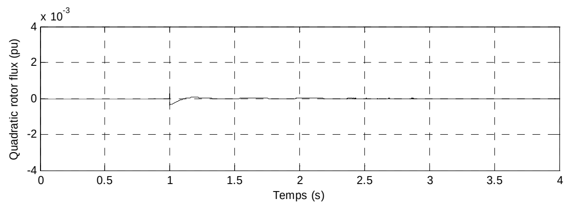

Fig. 12 Quadratic rotor flux

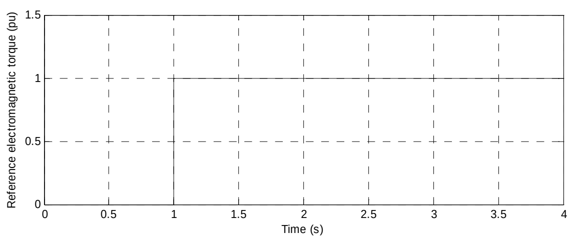

Fig. 13 Reference electromagnetic torque

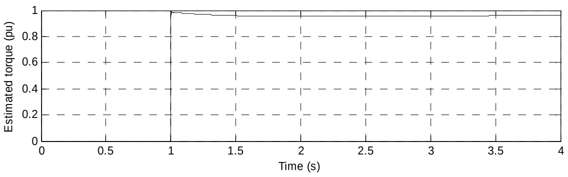

Fig. 14 Estimated electromagnetic torque

V. CONCLUSION

The work here presented leads to the development of an IRFOC drive scheme for an isolated wind turbine water pumping system.

Wind turbine coupled to a Self excited induction generator has been found suitable for remote area application and for energy saving. A diode rectifier and an inverter are used to adapt the supply conversion an order to perform the IRFOC induction motor drive.

The buck converter provides a stepped-down voltage to the load when DC bus voltage stepped-up in order to adapt the required voltage load against wind variation.

Simulation results are presented highlighting the overall proposed good performances of the system. These promising results open the possibility for the reconstitution of the proposed scheme to be set up for an on-line implementation.

TABLE I. SEIG-WIND TURBINE SYSTEM PARAMETERS

Nominal wind speed	9 m/s	Rotor resistance Rr	3.59 Ω
Rotor Turbine Diameter	4 m	Stator inductance Ls	0.0168 H
Nominal Voltage	220 V	Rotor inductance Lr	0.0168 H
Nominal current IN	3.5 A	Magnetisation inductance Msr	0.664 H
Stator resistance Rs	6.29 Ω	Pole pairs p	2

TABLE II. IM PARAMETERS

Stator resistance Rs	9.65 Ω	Magnetisation inductance Msr	0.4475 H
Rotor resistance Rr	4.305 Ω	Pole pairs p	2
Stator inductance Ls	0.4728 H	Nominal current IN	3.5 A
Rotor inductance Lr	0.4718 H		

REFERENCES

[1] N. Hidouri, S. Hammadi, L. Sbita, "An Advanced DPC-Self Excited Induction Generator Drive Scheme for an Isolated Wind turbine Boost System," International Review on Modelling and Simulations (IREMOS), vol. 5, no. 2, pp. 913-920, 2012.

[2] A.H.M.A Rahim, M. Ahsanul Alam, M.F. Kandlawala, Dynamic performance improvement of an isolated wind turbine induction generator, Computer and electric Engineering, vol. 35, no. 4, pp. 594-607, 2009.

[3] B mokhtari, A. Cheknane, A. Ameur, L. Mokrani et B. Azoui, "DTC d'un MAS utilisé pour l'optimisation des performances d'un panneau photovoltaique," , Revue des Energies Renouvelables, Vol. 11, no. 4, pp 595-602, 2008.

[4] Tomás Perpétuo Corrêa, Seleme Isaac Seleme Jr., Selênio Rocha Silva, "Efficiency optimization in stand-alone photovoltaic pumping system", Renewable Energy, vol. 41, pp. 220-226, 2012.

[5] Y.Inoue, S.Morimoto, M.Sanada, Control method for direct torque controlled PMSG in wind power generation system, Electric Machines and Drives Conference, IEEE International Electric Machines & Drives Conference, pp.1231-1238, 2009.

[6] Hong-Geuk Park, Dong-Choon Lee and Heung-Geun Kim, Cost-Effective Converters for Micro Wind Turbine Systems using PMSG, Journal of Power Electronics, vol. 8, no. 2, pp.156-162, 2008.

[7] P. Camorcadi, P. Battaiotto, R. Mantz, Autonomous BDFIG Wind generator with torque and pitch control for maximum efficiency in a water pumping system, International Journal of Hydrogen Energy, vol.35, pp. 5778-5785, 2010.

[8] S. Arnalte, J. C. Burgos, J. L. Rodrguez-Amenedoguez-Amenedo, Direct Torque Control of a Doubly-Fed Induction Generator for Variable Speed Wind Turbines, Electric Power Components and Systems, vol 30, no.2, pp. 199-216, 2002.

[9] Xing Zuoxia, Yao Xingjia, Sui Hong xia, Zheng, DTC in Doubly-fed VSCF wind turbine control system, Industrial Technology, IEEE International Conference on Industrial Technology, pp.2715-2718, 2006.

[10] S. Hammadi, N. Hidouri, L. Sbita, "A DTC-DFIG Drive Scheme for an Isolated Wind turbine Buck System," 10th International Multi-Conference on Systems, Signals & Devices SSD-13, march, 2013.

[11] S. Hammadi, N. Hidouri, L. Sbita, "A DTC-Induction-Generator drive scheme for an isolated wind turbine system," 16th IEEE Mediterranean Electrotechnical Conference (MELECON 2012), Medina Yasmine Hammamet Tunisia, march, 2012.

[12] N. Hidouri , L. Sbita, "A New DTC-SPMSM Drive Scheme for PV Pumping System," International Journal of Systems Control, vol.1, no.3, pp. 113-121, 2010.

[13] K. Raggl, B. Warberger, T. Nussbaumer, S. Burger, J. W. Kolar, "Robust Angle-Sensorless Control of a PMSM Bearingless Pump," IEEE Transactions on industrial electronics, Vol. 56, no. 6, pp. 2076-2085, 2009.

[14] Deokar, S.A., Waghmare, L.M., Jadhav, G.N., Voltage flicker assessment of induction motors used in the integrated water pumping station, International Conference on Power Electronics, Drives and Energy Systems & 2010 Power India

[15] M. Makhlouf, F. Messai, H. Benalla, "vectored command of induction motor pumping system supplied by photovoltaic generator," Journal of Electrical Engineering, vol. 62, no. 1, pp. 3–10, 2011.

[16] F. BLASCHKE, "The principle of field orientation as applied to the new transvector closed-loop control system for rotating-field machines," Siemens Review, vol. 39, No 5, pp. 217-220, 1972.

[17] S. peresada, A. Tonielli, R. Morici, "High - performance indirect field-oriented output-feedback control of induction motors," Automatica, vol 35, pp. 1033-1047, 1999.

[18] H. Rehman, A. Dhouadi, "A Fuzzy learning-sliding mode controller for direct field-oriented induction machines," Neurocomputing vol.71, pp. 2693-2701, 2008.

[19] M. M. Neam, Fayez F. M. El-Sousy, M. A. Ghazy and M.A. Abu-Adma, "DC-Bus Voltage Control of Three-Phase AC/DC PWM Converters for Renewable Energy Applications," International Electric Machine and Drives Conference (IEMDC09), Florida USA, May 3-6, 2009.

[20] Y. errami, M. Ouassaid, M. Maaroufi, "Control of grid connected PMSG based variable speed wind energy conversion system," International Review on Modelling and Simulations (IREMOS), vol. 5, no.2, pp. 655-664, April 2012.

[21] M. M. Aly, "Transient stability analysis of fixed speed wind turbines under constant and variable wind speeds using resistive superconducting fault current limiter," International Review on Modelling and Simulations (IREMOS), vol. 5, no.2, pp. 665-671, April 2012.